Quantitative Assessment of Artifacts on Cardiac Magnetic Resonance Imaging of Patients With Pacemakers and Implantable Cardioverter-Defibrillators

Takeshi Sasaki, MD; Rozann Hansford, RN, MPH; Menekhem M. Zviman, PhD; Aravindan Kolandaivelu, MD; David A. Bluemke, MD, PhD; Ronald D. Berger, MD, PhD; Hugh Calkins, MD; Henry R. Halperin, MD, MA; Saman Nazarian, MD

Background—The safety and clinical utility of MRI at 1.5 T in patients with cardiac implantable devices such as pacemakers (PM) and implantable cardioverter-defibrillators (ICD) have been reported. This study aims to evaluate the extent of artifacts on cardiac magnetic resonance (CMR) in patients with PM and ICD (PM/ICD).

Methods and Results—A total of 71 CMR studies were performed with an established safety protocol in patients with prepectoral PM/ICD. The artifact area around the PM/ICD generator was measured in all short-axis (SA), horizontal (HLA), and vertical long-axis (VLA) SSFP cine planes. The location and extent of artifacts were also assessed in all SA (20 sectors per plane), HLA, and VLA (6 sectors per plane) late gadolinium-enhanced CMR (LGE-CMR) planes. The artifact area on cine CMR was significantly larger with ICD versus PM generators in each plane ($P<0.001$, respectively). In patients with left-sided ICD or biventricular ICD systems, the percentages of sectors with any artifacts on LGE-CMR were 53.7%, 48.0%, and 49.2% in SA, HLA, and VLA planes, respectively. Patients with left-sided PM or right-sided PM/ICD had fewer artifacts. Anterior and apical regions were severely affected by artifact caused by left-sided PM/ICD generators.

Conclusions—In contrast to patients with right-sided PM/ICD and left-sided PM, the anterior and apical left ventricle can be affected by susceptibility artifacts in patients with left-sided ICD. Artifact reduction methodologies will be necessary to improve the performance of CMR in patients with left sided ICD systems. **(*Circ Cardiovasc Imaging*. 2011;4:662-670.)**

Key Words: MRI ■ artifacts ■ pacemakers ■ implantable cardioverter-defibrillator

The clinical utility and safety of noncardiac and cardiac MRI at 1.5 T in patients with cardiac implantable devices such as pacemaker (PM) and implantable cardioverter-defibrillator (ICD) systems has been investigated in previous reports.[1–12] Cardiac MRI (CMR) can be instrumental for the diagnosis of underlying cardiomyopathies, assessment of cardiac function and myocardial viability, assessment of disease progression, and identification of arrhythmogenic substrates.[12–23] However, many patients with cardiac pathology who would otherwise derive benefit from CMR will have received a cardiac device before referral for imaging. We previously found that metallic PM and ICD (PM/ICD) can produce susceptibility artifacts caused by distortion of MRI magnetic field resulting in bright and dark artifacts surrounding the generator and leads.[7] Consequently, the risk to benefit ratio of performing CMR in the setting of PM/ICD may be significantly altered compared with patients with PM/ICD who require noncardiac MRI.[1–8,24] We sought to quantitatively assess susceptibility artifacts on 1.5-T CMR, using our previously reported safety protocol for patients with PM/ICD.[1–3]

Clinical Perspective on p 670

Methods

The study protocol was reviewed and approved by the Johns Hopkins Institutional Review Board. Written informed consent was obtained from all patients after potential risks of PM/ICD exposure to MRI scanning were explained.

Device Safety Protocol for CMR in Patients With PM/ICD

Patients were enrolled if they had a clinical necessity for CMR, no acceptable imaging alternative, and PM/ICD was found to be safe by previous in vivo or in vitro testing.[1–3] Patients with device implantation <6 weeks before CMR and those with epicardial and abandoned leads were excluded. Specific device models included Medtronic EnTrust (T154ATG), GEMIII (7231), Insync (7272), Marquis (7274), Maximo (7232, 7278), Virtuso (D154AWG, D154VRC); Boston Scientific Confient (E030), Contak Renewal (H119, H170, H175,H210, H217, H219), Ventak Prizm (1852, 1860, 1861), Vitality (T125, T135, T165, T167, T175, T177); and St Jude Medical Atlas (V343, V366), Current (1207-36), Promote (3207-36) ICD, and BiV-ICD devices. Addition-

Received April 24, 2011; accepted September 21, 2011.

From the Department of Medicine/Cardiology, Johns Hopkins University School of Medicine, Baltimore, MD (T.S., R.H., M.M.Z., A.K., R.D.B., H.C., H.R.H., S.N.); and Radiology and Imaging Sciences, NIH Clinical Center, National Institute of Biomedical Imaging and Bioengineering, Bethesda, MD (D.A.B.).

The online-only Data Supplement is available at http://circimaging.ahajournals.org/lookup/suppl/doi:10.1161/CIRCIMAGING.111.965764/-/DC1.

Correspondence to Takeshi Sasaki, MD, Johns Hopkins University, Division of Cardiology, Carnegie 592C, 600 N Wolfe St; Baltimore, MD 21287. E-mail tsasaki1@jhu.edu

ally, the following PM models were included: Medtronic EnPulse (E2DR01, E2DR21), Kappa (KDR401, KDR701, KDR901); Boston Scientific Insignia (1290); St Jude Medical; Identity (5376, 5386), Integrity (5142, 5342, 5346), and Trilogy (2360). Device interrogation to assess parameters including battery voltage, lead impedance, lead capture thresholds, and sensing were performed immediately before, immediately after, and at routine clinic follow-up. Pacing mode was programmed to asynchronous in PM-dependent patients without a hemodynamically stable escape rhythm, whereas the patients without PM dependence were programmed to the ventricular or dual-chamber inhibited pacing mode. Magnet response, noise response, ventricular sense response, conducted atrial fibrillation response, and tachyarrhythmia functions (monitoring, antitachycaradia pacing, and defibrillation) were turned off before CMR. Devices were reprogrammed to original settings after the completion of CMR. Blood pressure, ECG telemetry, pulse oximetry, and symptoms were monitored. In addition, a registered nurse trained in advanced cardiac life support and familiar with device programming and trouble shooting was present at all CMR scans. The specific absorption rate (SAR) of MRI sequences was limited to less than 2.0 W/kg during our initial experience (27/71 CMR studies).[1] After the initial period, given the lack of association between SAR and device parameter changes[10,11] and the unreliability of using SAR to guide MRI safety recommendations,[12] no restrictions beyond standard manufacturer SAR limits were applied in subsequent patients.

Cardiac MRI

CMR scans were performed with a 1.5-T scanner (Avanto, Siemens Medical Systems, Malvern, PA) with maximum gradient field 45 mT/m and slew rate 200 T/m/s. ECG telemetry, pulse oximetry, blood pressure, and symptoms were monitored during the scan. Cine steady-state free precession (SSFP) gradient-echo images were obtained in multiple short axis (SA), horizontal long axis (HLA) and vertical long axis (VLA) planes (echo time, 1.1–1.6 ms; repetition time, 2.5–3.8 ms; average in-plane resolution, 1.4×1.4 mm^2; flip angle, 45–60°; temporal resolution, 40–45 ms). Fifteen minutes after bolus injection of 0.2 mmol/kg intravenous gadolinium contrast, late gadolinium-enhanced CMR (LGE-CMR) was obtained in 10–13 SA planes with an inversion-recovery fast-gradient-echo pulse sequence (echo time, 1.3–3.9 ms; repetition time, 5.4–8.3 ms; average in-plane resolution, 1.5×2.0 mm^2; 8-mm slice thickness; flip angle, 30°). Inversion times (range, 175–300 ms) were optimized for each patient to maximize conspicuity of myocardial delayed enhanced area. Single planes of LGE-CMR were also acquired in VLA and HLA planes. In a subgroup of patients, three T2-weighted SA planes acquired by a T2-weighted turbo spin echo sequence before contrast administration (echo time, 76 ms; repetition time, 1800–2100 ms; average in-plane resolution, 1.4×1.4 mm^2; 10-mm slice thickness; flip angle, 180°), and first-pass myocardial perfusion imaging using hybrid fast gradient echo/echo planar technique in 4 SA planes (echo time, 1.0–1.1 ms; repetition time, 164–256 ms; average in-plane sequence, 1.9×1.9 mm^2; 8-mm slice thickness; flip angle, 12°) were also performed. Contrast-enhanced MR angiography was additionally performed in a subgroup of patients before and immediately after contrast agent administration (echo time, 1.0–1.1 ms; repetition time, 2.7–2.9 ms; average in-plane sequence, 1.0×1.0 mm^2; 1-mm slice thickness; flip angle, 25°).

Measurements of Artifact Caused by PM/ICD

The maximum area of image susceptibility artifact was measured in SA, HLA, and VLA planes on cine CMR, and the percentage of cine CMR scans with any artifacts was also assessed in the three different planes (Figure 1A). The artifact size and the percentage of cine CMR scans with any artifacts in each plane were compared between patients with ICD/BiV-ICD and those with PMs. The association of artifact size with generator dimensions (area defined as height×width, thickness, weight, and volume) was evaluated. The feasibility of cardiac function calculation based on cine CMR (ie, clear visualization of myocardial borders free from artifact) was also evaluated in the four groups divided by the type of cardiac devices (ICD/BiV-ICD, PM) and the implanted side of device generator (left, right). The extent of artifacts on LGE-CMR in SA, HLA and VLA planes was recorded. To ascertain regional differences in artifact, the left ventricular myocardium was divided into 20 sectors in each SA plane and 6 sectors in each single HLA and VLA planes (Figure 1B). The percentage of sectors with/without artifact in the three different planes was assessed in the 4 groups described above. The percentage of sectors with artifact was summarized using the 17-segment model. The extent of artifacts in SA planes of cine CMR was assessed in the same way as the analysis of LGE-CMR. The distance from the generator to the cardiac silhouette on antero-posterior (AP) chest radiography was measured (if the generator border overlapped the cardiac silhouette the distance was reported as 0), and the association between that distance and the percentage of sectors with artifact in SA, HLA, and VLA planes was assessed. In patients with left-sided ICD/BiV-ICD, the artifact effects on cine, T2-weighted, perfusion, and LGE-CMR images were compared. Finally, artifact effects caused by PM/ICD leads were assessed by measuring the area of artifact surrounding the lead tip in SA cine CMR images. The artifact area surrounding PM/ICD leads was also measured in SA planes of cine CMR at the tip of the lead. In a subgroup of patients who had previously undergone cardiac computed tomography (CT), artifact characteristics were qualitatively compared between MRI and CT. Cardiac CT images were acquired using a 64-slice CT scanner (Aquillon, Toshiba Medical Systems Corporation, Tochigi, Japan). Image acquisition was performed during 1 breath-hold at the end-expiratory phase. The duration of scanning was approximately 10 seconds and scanning was retrospectively gated to the cardiac cycle. CT images were reconstructed every 10% of the cardiac cycle with a slice thickness of 1 mm.

Interpretability of CMR Images

The percentage of image series qualitatively defined as "successfully interpretable," "partially interpretable," and "impossible to interpret" for each of 4 pulse sequences (LGE-CMR, cine CMR, perfusion CMR, and MR angiography) were calculated and stratified by location of device and underlying heart disease. All images were reviewed by 2 independent observers, and discrepancies (<5 cases) were resolved by the senior observer.

Statistical Analysis

All values are expressed as mean±SD. Comparisons of continuous variables were made using Student *t* test, and categorical variables were compared with χ^2 testing or Fisher exact test where appropriate. Spearman rank correlation test was used to assess the association between artifact size and parameters related to generator dimensions. Linear regression analysis was used to assess the relationship between the minimum distance from PM/ICD generator to heart on frontal chest radiography and percent sectors with artifact caused by the PM/ICD generator on LGE-CMR. All tests were 2-tailed, and analyses were performed using STATA 10 statistical software (StataCorp, College Station, TX).

Results

A total of 71 CMR examinations were performed in 66 patients with PM/ICD between November 2003 and March 2010. Of 71 scans, 56 (78.9%) were acquired in patients with ICD or biventricular ICD (BiV-ICD) systems, and 15 (21.1%) were acquired in patients with PM systems. All ICD/BiV-ICD systems were implanted in the left infraclavicular prepectoral area except 1 BiV-ICD, and 4 PMs, which were implanted in the right infraclavicular prepectoral area. Patient characteristics are summarized in Table 1. Patients with ICD devices were older and more likely to have structural heart disease than those with PMs. Body mass index (BMI) was similar between the 2 groups. Patient safety issues have been reported separately.[1]

The estimated whole-body averaged SAR in each image acquisition sequence is reported in online-only Data Supplement Figure I. No clinically significant PM/ICD parameter changes requiring system revision or reprogramming were noted after CMR. The clinical indications for CMR studies

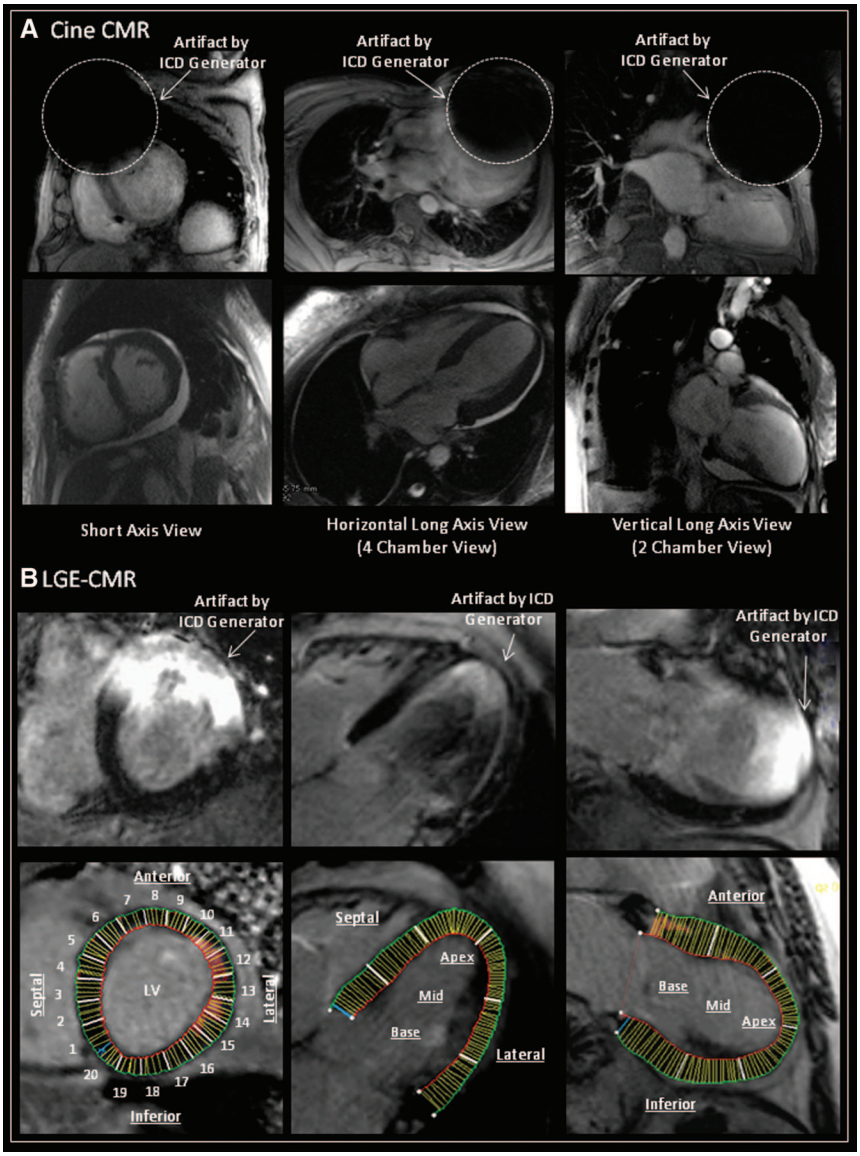

Figure 1. Methodology for measurement of artifacts on cine cardiac magnetic resonance imaging (CMR) and late gadolinium-enhanced CMR (LGE-CMR). Artifact size on steady-state free precession (SSFP) cine and LGE-CMR was measured in short-axis (SA), horizontal long-axis (HLA), and vertical long-axis (VLA) planes. **A**, The artifact size on cine CMR caused by the pacemaker and implantable cardioverter-defibrillator (PM/ICD) was measured. Percent sectors with any artifacts on cine CMR were also assessed in each plane. **B**, The regional artifact effects on LGE-CMR caused by the generator were quantitatively estimated in each plane (divided into 20 sectors in SA, 6 sectors in HLA, and 6 sectors in VLA planes, respectively).

were as follows: (1) general assessment of myocardial function and viability in patients with underlying heart disease (26 scans; 37%); (2) diagnosis of suspected cardiac conditions (arrhythmogenic right ventricular cardiomyopathy, cardiac sarcoidosis, myocarditis, etc) (7 scans; 10%); (3) preoperative evaluation of cardiac function, viability, and anatomy (before coronary artery bypass grafting, left ventricular plasty for ischemic left ventricular aneurysm, valve surgery, heart transplant, radiofrequency catheter ablation, or device upgrade to BiV-ICD) (27 scans; 38%); and (4) postoperative evaluation (coronary artery bypass grafting, valve surgery, or congenital heart disease) (11 scans; 15%).

Artifact Size on Cine CMR

Artifact sizes in SA, HLA, and VLA planes on cine CMR has been shown in the online-only Data Supplement Table. Susceptibility artifacts were present on cardiac cine CMR in 100% of SA planes, 26.9% of HLA planes, and 76.1% of VLA planes in patients with left- and right-sided ICD/BiV-ICD systems. In contrast, artifacts were observed in 93.3% of SA planes, 23.1% of HLA planes, and 33.3% of VLA planes in patients with left- and right-sided PM systems. Artifacts were more likely to be present on SA planes compared with HLA planes ($P=0.0001$). In VLA planes of cine CMR, artifacts were more common in patients with ICD/BiV-ICD than those with PMs ($P=0.012$). The artifact size on every plane of cine CMR was significantly greater in patients with ICD/BiV-ICD compared with those with PM. Artifacts size in patients with ICD/BiV-ICD systems was significantly smaller in HLA planes than in SA or VLA planes ($P<0.0001$). Online-only Data Supplement Figure II illustrates the correlation between artifact size in each plane and generator dimensions. The artifact area surrounding the tip of PM/ICD leads on cine CMR averaged 1.05 ± 0.35 cm^2 and 1.09 ± 0.38 cm^2 for PM and ICD leads, respectively.

Artifact Effects on Cardiac Function Evaluation by Cine CMR

CMR images of patients with left-sided ICD/BiV-ICD systems had more artifact effects on SA plane of cine CMR compared with those in patients with left-sided PM and right-sided PM/

Table 1. Baseline Characteristics

	ICD/BiV-ICD (n=56 Scans)	PM (n=15 Scans)	*P* Value
Age	59±15	43±16	0.001
Female/male	8/48	7/8	0.012
ICD/BiV-ICD	42 ICD/14 BiV-ICD	(. . .)	
Generator left-sided/ right-sided	55/1	11/4	0.006
Structural heart disease	56	13	0.042
ICM/NICM/HCM/ congenital/other	38/16/1/0/1	0/7/1/6/1	<0.0001
Body weight, kg	81.6±16.5	70.3±15.3	0.034
Body height, cm	176.8±8.8	166.8±16.0	0.056
Body mass index, kg/m^2	26.0±4.0	25.4±5.3	0.688
Ejection fraction, %	34.0±15.9	51.5±16.5	0.002
LVEDD, mm	56.8±10.8	45.4±5.6	0.006
Possible cardiac function evaluation by cine CMR	47/55 (85.5%)	15/15 (100%)	0.266
Patients with CT data	22 (39.3%)	4 (26.7%)	0.548
Generator size			
Height, mm	68.8±6.6	46.7±3.8	<0.0001
Width, mm	56.2±5.7	46.7±4.4	<0.0001
Area, height×width, cm^2	38.7±7.1	21.7±2.0	<0.0001
Thickness, mm	13.1±1.8	6.9±0.9	<0.0001
Weight, g	81.5±8.9	24.3±1.8	<0.0001
Volume, mL	36.4±6.0	11.3±0.9	<0.0001

ICD indicates implantable cardioverter-defibrillator; BiV-ICD, biventricular ICD; ICM/NICM/HCM, ischemic/nonischemic/hypertrophic cardiomyopathy; LVEDD, left ventricular end-diastolic diameter; CMR, cardiac magnetic resonance; and CT, computed tomography.

Values are mean±SD.

Table 2. Predictor of Cardiac Function Evaluation by Cine CMR

	Cardiac Function Evaluation by Cine CMR in Patients With Left-Sided ICD/BiV-ICD		
	Possible (n=47 Scans)	Impossible (n=8 Scans)	*P* Value
Age	58±14	64±20	0.27
Female/male	7/39	1/7	0.84
Body mass index, kg/m^2	26.9±3.9	23.1±2.8	0.019*
Ejection fraction, %	34.0±16.1	34.0±17.1	0.996
Left ventricular end-diastolic diameter, mm	55.3±10.8	65.0±7.7	0.045*
Artifact size on short axis of cine MRI, cm^2	200.3±32.4	186.6±19.7	0.478
Minimum distance from generator to heart, mm			
Frontal chest radiography	31.7±20.9	15.7±15.0	0.08
Lateral chest radiography	32.2±4.0	33.2±3.6	0.58
Generator			
Height×width, cm^2	38.7±6.4	39.2±7.5	0.82
Thickness, mm	13.0±1.8	13.0±1.7	0.99
Weight, g	80.6±8.3	81.5±7.2	0.78
Volume, mL	36.1±5.9	35.1±5.0	0.65

CMR indicates cardiac magnetic resonance; ICD, implantable cardioverter-defibrillator; and BiV-ICD, biventricular ICD.

Values are mean±SD or number.

*Significant, $P<0.05$.

ICD (18.9% versus 0%, $P<0.0001$, respectively) (online-only Data Supplement Figure III, A). The anterior region on SA planes of cine CMR were more likely to be affected by artifact than other regions ($P<0.0001$) (online-only Data Supplement Figure III, B). Severe artifacts observed in more than half of the myocardial sectors on cine CMR precluded accurate cardiac function evaluation in 8 scans (14.5%). In contrast, it was possible to evaluate cardiac function by cine CMR in 47 of 55 CMR scans (85.5%) in the setting of left-sided ICD/BiV-ICD systems and all CMR scans (16 scans) in patients with left-sided PM and right-sided PM/ICD. Patients in whom cardiac function evaluation was possible had higher BMI and greater left ventricular end-diastolic diameter (LVEDD) compared with those in whom cardiac function could not be calculated ($P=0.019$ for BMI, $P=0.045$ for LVEDD, Table 2).

Artifact Effects on LGE-CMR

In patients with left-sided ICD/BiV-ICD systems, artifacts on LGE-CMR were observed in 4501 of 8379 sectors (53.7%) in SA planes, 147 of 306 sectors (48.0%) in HLA planes, and 124 of 252 sectors (49.2%) in VLA planes. On the other hand, no artifact on LGE-CMR was confirmed in HLA and VLA planes in patients with left-sided PM or any planes in patients with right-sided ICD/BiV-ICD systems. Only 146 of 1493 sectors (9.8%) in SA planes had artifacts in patients with left-sided PM (Figure 2A). The characteristic distribution of artifacts in patients with left-sided ICD/BiV-ICD devices is summarized in Figure 2B. The anterior regions were more affected by artifact caused by the ICD/BiV-ICD generator in SA planes. The apical myocardial regions were also influenced by the artifact compared with basal regions in HLA planes. In VLA planes, the anterior apical regions were severely affected by the artifact. In comparison with left-sided ICD/BiV-ICD systems, fewer sectors needed to be excluded due to artifacts of left-sided PM generators (Figure 2C). The percentages of sectors with artifacts on LGE-CMR are summarized by the 17-segment model (Figure 3). The mean distance from PM/ICD generator to the silhouette of heart on AP chest radiography was 24.8±16.5 (range, 0—57) mm in patients with left-sided ICD/BiV-ICD and 29.3±20.5 (0–44.6) mm in left-sided PM. The distance from generator to heart was significantly associated with the percentage of the sectors with artifacts on LGE-CMR in each plane ($R^2=0.474$, $P<0.0001$ in SA planes; $R^2=0.566$, $P<0.0001$ in HLA planes; $R^2=0.391$, $P=0.0001$ in VLA planes). The artifacts caused by PM/ICD leads were much smaller than those caused by the PM/ICD generators. Fewer artifact effects caused by the PM/ICD leads were observed regardless of the image sequence and type of PM/ICD leads such as ICD, PM, or coronary sinus leads.

Comparisons of Artifact Effects on Cine CMR, LGE-CMR, T2-Weighted, and Perfusion CMR Images

Of 55 patients with left-sided ICD systems, 13 patients (23.6%) underwent all T2-weighted, perfusion, cine, and

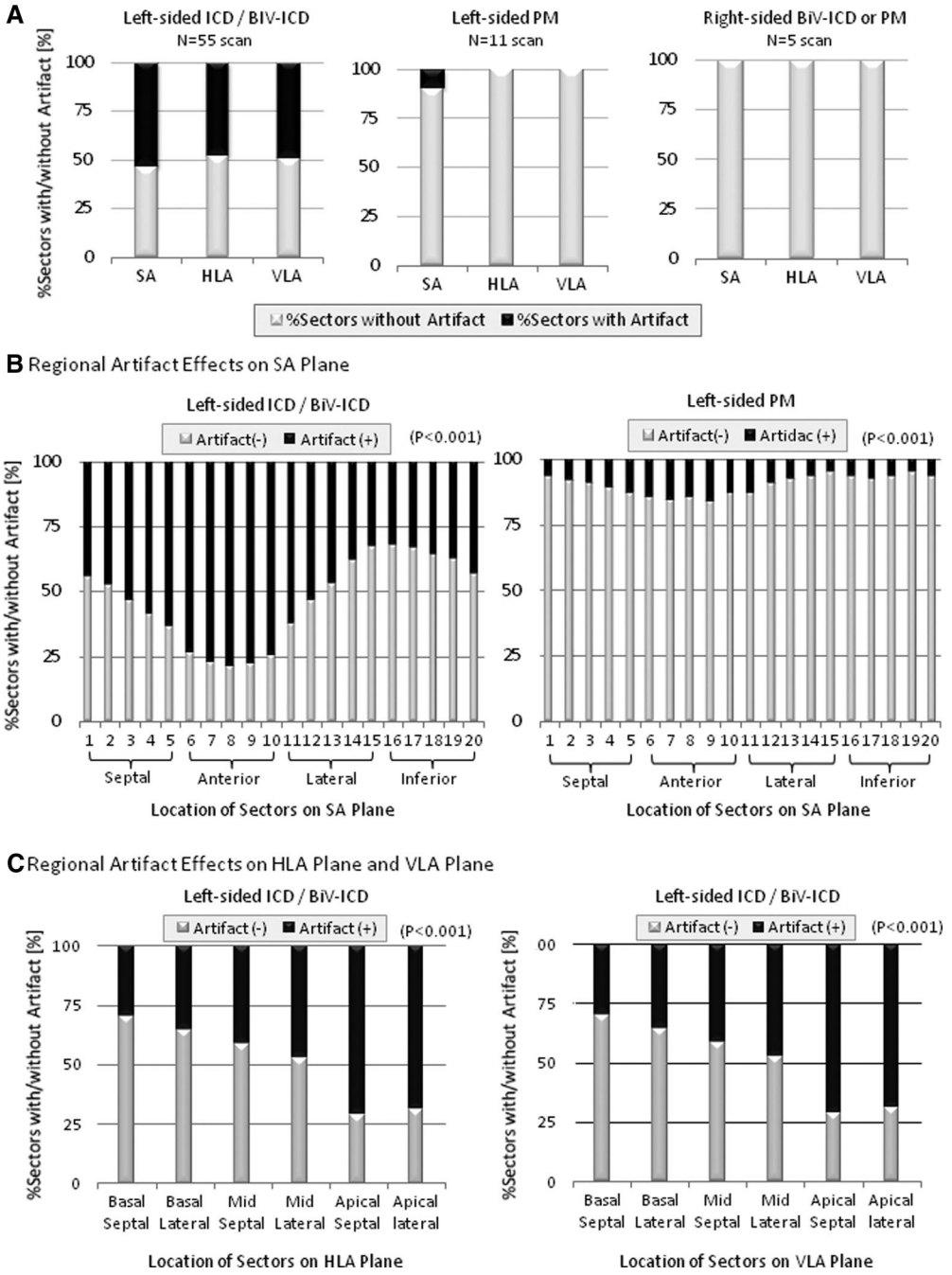

Figure 2. Artifact effects on late gadolinium-enhanced cardiac magnetic resonance imaging (LGE-CMR). Artifact effects in each plane of LGE-CMR caused by the generator were quantitatively assessed in patients with left- and right-sided implantable cardioverter-defibrillator (ICD)/biventricular (BiV)-ICD or pacemaker (PM) systems. **A**, The greatest artifact on LGE-CMR was observed in patients with left-sided ICD/BiV-ICD. About 50% of the sectors were affected by the artifact. **B**, Details about the regional artifact effects on short-axis (SA) planes are demonstrated in patients with left-sided ICD/BiV-ICD and PM systems. The anterior and apical regions were severely affected by artifacts caused by the generator in patients with ICD/BiV-ICD systems. Smaller artifacts were observed in patients with left-sided PM systems. **C**, The regional artifact effects on HLA and VLA plane are shown in patients with left-sided ICD/BiV-ICD systems. The apical regions on HLA and VLA planes were severely affected by the artifact.

LGE-CMR sequences. Artifact effects on the three corresponding SA planes of cine, T2-weighted, perfusion, and LGE-CMR images were compared in each myocardial region such as septal, anterior, lateral and inferior regions (Figure 4). Compared with other image sequences, susceptibility artifacts due to the ICD/BiV-ICD generator were most extensive on LGE-CMR and affected all regions except the inferior wall (LGE-CMR versus cine CMR, T2-weighted, and perfusion CMR in septal, anterior, and lateral myocardial regions; $P<0.001$, respectively). Most artifacts on T2-weigthed images were caused by cardiac motion or arrhythmia rather than the susceptibility artifacts from the PM/ICD generator.

Interpretability of CMR Images

The percentages of cine, perfusion, LGE-CMR, and MR angiography sequences with interpretable images are summa-

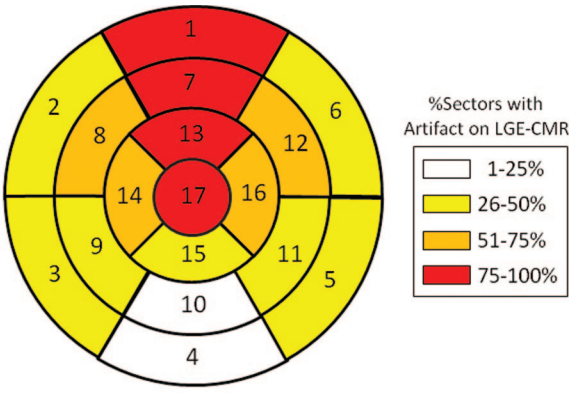

Figure 3. Seventeen-segment model of artifact effects on late gadolinium-enhanced cardiac magnetic resonance imaging (LGE-CMR). Artifact effects on LGE-CMR in patients with left-sided sided implantable cardioverter-defibrillator/biventricular ICD are summarized using the 17-segment model. The percentages of sectors with artifact on LGE-CMR were divided into 4 groups (1–25%, 26–50%, 51–75%, and 76% to 100%).

rized in Table 3. All CMR images were interpretable in patients with PM and right-sided ICD systems (16/16 scans; 100%). In contrast, interpretability of CMR images in patients with left-sided ICD/BiV-ICD systems was dependent on the extent of susceptibility artifacts due to PM/ICD generators. Despite the presence of some artifact in most image sequences, images were completely (18/55 scans; 32.7%) or partially (31/55 scans, 56.4%) interpretable in most patients with left-side ICD/BiV-ICD systems.

Discussion

Despite prior demonstration of overall safety, MRI in the setting of PM/ICD systems may be associated with risks including heating, current induction leading to arrhythmia, generator movement, and/or PM/ICD malfunction.[1–12] Therefore, the risks of CMR must be weighed against the potential clinical utility of images to be acquired in each case. By reporting the extent of artifact in each sequence and associations with generator size, location, and patient characteristics, this study enables improved patient selection for CMR. The extent of each plane involved by artifact on cine CMR was dependent on the imaging plane. Artifacts were more pronounced in the SA plane compared with HLA and VLA planes, largely because of the proximity between the PM/ICD generator and affected regions of the heart in each plane. Artifact size on cine CMR was also significantly associated with the size of the PM/ICD generator. We found that the artifact size due to ICD/BiV-ICD devices was greater than that with PM devices in proportion to the size of PM/ICD generator. It was possible to evaluate cardiac function using cine CMR in 86% of patients with left sided ICD. The most significant predictors of the capability to assess cardiac function were BMI and LVEDD. Both associations are probably mediated by the distance between the PM/ICD generator and the heart. Scans with right-sided ICD/BiV-ICD and PM systems had no effects on LGE-CMR images. In

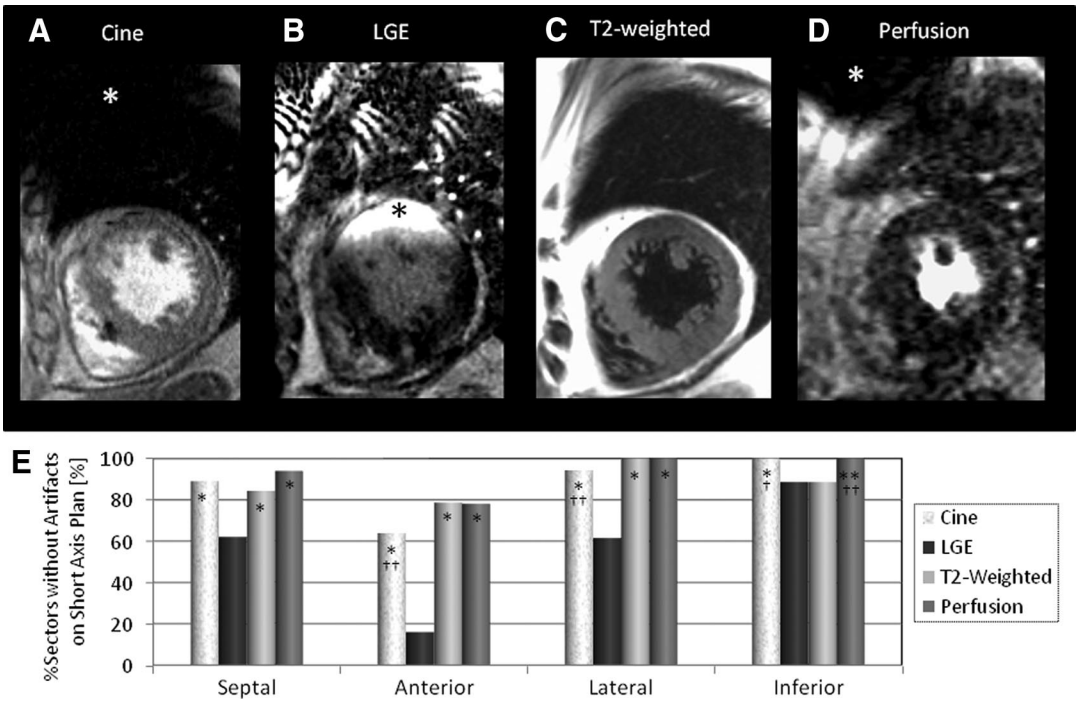

Figure 4. Comparison of artifact effects on cine, T2-weighted, perfusion, and late gadolinium-enhanced cardiac magnetic resonance imaging (LGE-CMR). Comparison of artifact distribution and extent (asterisks) caused by the implantable cardioverter-defibrillator generator on **A**, cine CMR; **B**, LGE-CMR; **C**, T2-weigthed; and **D**, perfusion CMR images. **E**, Percentage of the sectors without any artifacts on short-axis planes in each image sequence. Artifact effects on LGE-CMR images were greater compared with the other images in all except the inferior myocardial regions (LGE-CMR versus cine, T2-weighted, and perfusion CMR in the septal, anterior, and lateral myocardial regions; $P<0.001$, respectively). *$P<0.001$ versus LGE-CMR, **$P<0.01$ versus LGE-CMR, †$P<0.001$ versus T2-weighted CMR; ††$P<0.01$ versus T2-weighted CMR.

Table 3. Percentages of Scans With Interpretable Images in Patients With Cardiac Implantable Devices

Underlying Heart Disease	Patient No.	Interpretable Images, %										
		LGE-CMR (n=71 Scans)			Cine CMR (n=71 Scans)			Perfusion CMR (n=36 Scans)			MR Angiography (n=32 Scans)	
		◎	Δ	×	◎	Δ	×	◎	Δ	×	◎	×
Left-sided ICD/BiV-ICD												
Ischemic cardiomyopathy												
Anteroseptal MI	20	5	90	5	85	0	15	57	43	0	100	0
Inferior MI	14	0	85	15	77	8	15	17	83	0	100	0
Diffuse	4	25	75	0	100	0	0	0	100	0	100	0
Dilated cardiomyopathy	10	10	80	10	100	0	0	0	50	50	100	0
ARVC	4	0	100	0	75	0	25	100	0	0	100	0
Cardiac sarcoidosis	2	0	100	0	100	0	0	100	0	0	100	0
Hypertrophic cardiomyopathy	1	0	100	0	100	0	0	100	0	0	100	0
Idiopathic ventricular tachycardia	1	100	0	0	100	0	0	(. . .)	(. . .)	(. . .)	(. . .)	(. . .)
Left-sided PM, right-sided PM/ICD												
Congenital heart disease	7	86	14	0	100	0	0	100	0	0	100	0
Myocardial dystrophy	3	67	33	0	100	0	0	67	33	0	(. . .)	(. . .)
Dilated cardiomyopathy	1	100	0	0	100	0	0	100	0	0	(. . .)	(. . .)
ARVC	1	100	0	0	100	0	0	100	0	0	(. . .)	(. . .)
Cardiac sarcoidosis	1	100	0	0	100	0	0	100	0	0	(. . .)	(. . .)
Hypertrophic cardiomyopathy	1	100	0	0	100	0	0	0	100	0	(. . .)	(. . .)
Neuromediated syncope	2	100	0	0	100	0	0	(. . .)	(. . .)	(. . .)	(. . .)	(. . .)

LGE-CMR indicates late gadolinium-enhanced cardiac magnetic resonance imaging; ICD, implantable cardioverter-defibrillator; BiV-ICD, biventricular ICD; MI, myocardial infarction; ARVC, arrhythmogenic right ventricular cardiomyopathy; and PM, pacemaker.

Values are shown as numbers or percentages. The interpretability of the CMR images was defined as completely interpretable (◎), partially interpretable (Δ), and impossible to interpret (×).

patients with left-sided ICD/BiV-ICD systems, the artifacts on LGE-CMR images were most often localized to the anterior and apical myocardial regions. The artifact effects on LGE-CMR were significantly greater than cine, T2-weighted, and perfusion CMR images in patients with left-sided ICD systems. T2-weighted images scanned by the turbo spin echo sequence had fewer susceptibility artifacts caused by PM/ICD generator compared with other image sequences.[25,26] Additionally, the distance between the PM/ICD generator and cardiac silhouette on frontal chest radiography (AP) was inversely associated with artifact size on LGE-CMR.

Artifact Effects on CMR Caused by PM/ICD Leads

Artifacts on CMR created by PM/ICD leads are smaller than those by PM/ICD generators. Artifacts caused by PM/ICD leads did not affect image interpretation in any patient regardless of the image sequence or the type of lead. The conducting wires and ICD coils of PM/ICD leads, although ferromagnetic, are thin and therefore associated with significantly less artifact compared with PM/ICD generators. In addition, the lead tips are made from nonferromagnetic materials such as platinum or other alloys that result in minimal artifact on CMR images. Artifacts of PM/ICD leads on cardiac CT are qualitatively larger than those on CMR (Figure 5).[27] Based on our experience, CMR appears to be the superior modality for evaluation of myocardium near PM/ICD leads (eg, to rule out perforation).

Mechanism of PM/ICD Artifacts on MRI

Metallic PM/ICD components have magnetic susceptibilities that are very different from human tissue. Such disparities in magnetic susceptibility lead to significant distortion of the MRI magnetic field and result in image artifacts (Figure 5). Various metallic PM/ICD components contribute differently to the observed artifact. For example, ferromagnetic components such as stainless steel made from iron alloys result in significantly larger artifacts than components made from materials such as titanium, which have much lower relative magnetic susceptibility.[25,26] The size and orientation of the artifact are associated with the direction and strength of the magnetic field, the relative magnetic susceptibility of the PM/ICD, and the type of pulse sequence being used. SSFP gradient echo and inversion recovery sequences with longer echo times are associated with increased magnetic susceptibility artifacts compared with gradient echo and spin echo sequences.[25,26] Artifacts caused by PM/ICD generators can be reduced by use of lower magnetic field strength and shorter echo times; however, such adjustments may compromise the image signal intensity and contrast. The use of spin-echo techniques produces black-blood contrast, which is not always desirable and is typically associated with high SAR, which may reduce safety.[1–12,24] Importantly, PM and ICD/BiV-ICD systems substantially differ from other metal implants such as orthopedic artificial joints[26] and dental im-

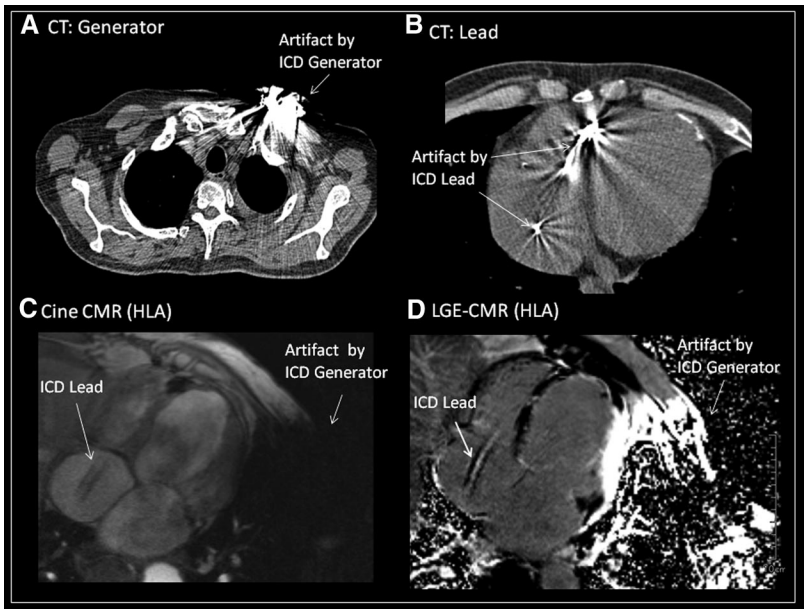

Figure 5. Artifact effects on late gadolinium-enhanced (LGE) cardiac magnetic resonance imaging caused by pacemaker and implantable cardioverter-defibrillator pacemaker/implantable cardioverter-defibrillator (ICD) leads. Comparison of artifacts caused by the ICD generator and lead in both computed tomography (CT) (**A** and **B**) and MRI (**C** and **D**) in a patient with single-chamber ICD. Artifacts caused by the lead were smaller on MRI compared with CT. In contrast, artifacts caused by the generator were larger with MRI.

plants.[28] PM/ICD are intricate electronic devices, and their dysfunction can be directly associated with life-threatening events. These limitations must be taken into account when adjusting parameters to reduce artifact size on CMR.

Study Limitations

In the current study, we analyzed the artifacts on the most commonly used sequences in CMR including SSFP cine, LGE, T2-weighted, perfusion, and contrast-enhanced MR angiography. Artifacts in other image sequences were not evaluated. Additionally, newer "MRI conditional devices" were not studied. However, the modifications incorporated into such systems primarily focuses on safety rather than artifact reduction. This study included only 1 patient with a right-sided BiV-ICD system; therefore, artifact effects in this setting could not be sufficiently evaluated. All PM/ICD generators were implanted in the infraclavicular prepectoral area; therefore, artifact effects due to submuscular devices were not investigated. Although interpretability was assessed by 2 independent observers and disagreements were rare, the measure is subjective and an interobserver reliability analysis was not performed. Distance between the generator and the cardiac silhouette on frontal chest radiography was considered the most readily available quantifiable parameter before CMR and was therefore used as predictor of artifact effects in this study. However, the distance on frontal radiography is a unidimensional surrogate of the true distance and 3D imaging techniques may improve the association.

Conclusions

This study demonstrated artifact characteristics on SSFP cine, T2-weighted, perfusion, LGE-CMR, and MR angiography in patients with PM/ICD. The utility of CMR in patients with left-sided ICD/BiV-ICD systems may be limited because of larger PM/ICD artifacts than in patients with PM or right-sided ICD/BiV-ICD systems. Artifact reduction methodologies for CMR in the setting of left-sided PM/ICD systems warrant further investigation.

Sources of Funding

Dr Sasaki is funded by the Francis Chiaramonte MD Private Foundation. Dr Nazarian is supported by Career Development Award K23HL089333 and Dr Halperin by grant R01-HL65795 from the National Institutes of Health.

Disclosures

Dr Nazarian received honoraria for lectures from St Jude Medical Inc, Boston Scientific Inc, and Biotronic Inc. Dr Halperin received research grant and consultant fees from Zoll Circulation Inc and has ownership interests in MRI International Inc and IMRICOR Medical Systems Inc. Dr Calkins received honoraria from Biosense Webster Inc and Medtronic Inc. Dr Berger received research grants from St Jude Medical Inc and Medtronic Inc and consultant fees from Boston Scientific Corp and Cameron Health Inc. The Johns Hopkins University Conflict of Interest Committee manages all commercial arrangements.

References

1. Nazarian S. Roguin A, Zviman MM, Lardo AC, Dickfeld TL, Calkins H, Weiss RG, Berger RD, Bluemke DA, Halperin HR. Clinical utility and safety of a protocol for noncardiac and cardiac magnetic resonance imaging of patients with permanent PMs and ICDs at 1.5 Tesla. *Circulation*. 2006;114:1277–1284.
2. Roguin A, Zviman MM, Meininger GR, Rodrigues ER, Dickfeld TM, Bluemke DA, Lardo A, Berger RD, Calkins H, Halperin HR. Modern PM and ICD systems can be magnetic resonance imaging safe: in vitro and in vivo assessment of safety and function at 1.5 T. *Circulation*. 2004;110:475–482.
3. Nazarian S, Halperin HR. How to perform magnetic resonance imaging on patients with implantable cardiac arrhythmia devices. *Heart Rhythm*. 2009;6:138–143.
4. Pulver AF, Puchalski MD, Bradley DJ, Minich LL, SU JT, Saarel EV, Whitaker P, Etheridge SP. Safety and imaging quality of MRI in pediatric and adult congenital heart disease patients with PMs. *Pacing Clin Electrophysiol*. 2009;32:450–456.
5. Naehle CP, Strach K, Thomas D, Meyer C, Linhart M, Bitaraf S, Litt H, Schwab JO, Schild H, Sommer T. Magnetic resonance imaging at 1.5-T in patients with ICDs. *J Am Coll Cardiol*. 2009;54:549–555.
6. Tian J, Smith MF, Jeudy J, Dickfeld T. Multimodality fusion imaging using delayed-enhanced cardiac magnetic resonance imaging, computed tomography, positron emission tomography, and real-time intracardiac echocardiography to guide ventricular tachycardia ablation in ICD patients. *Heart Rhythm*. 2009;6:825–828.
7. Roguin A, Donahue JK, Bomma CS, Bluemke DA, Halperin HR. Cardiac magnetic resonance imaging in a patient with ICD. *Pacing Clin Electrophysiol*. 2005;28:336–338.

8. Sommer T, Naehle CP, Yang A, Zeijlemaker V, Hackenbroch M, Schmiedel A, Meyer C, Strach K, Skowasch D, Vahlhaus C, Litt H, Schild H. Strategy for safe performance of extrathoracic magnetic resonance imaging at 1.5 Tesla in the presence of cardiac PMs in non-PM-dependent patients: a prospective study with 115 examinations. *Circulation*. 2006;114:1285–1292.
9. Levine GN, Gomes AS, Arai AE, Bluemke DA, Flamm SD, Kanal E, Manning WJ, Martin ET, Smith JM, Wilke N, Shellock FS. Safety of magnetic resonance imaging in patients with cardiovascular devices: an American Heart Association scientific statement from the Committee on Diagnostic and Interventional Cardiac Catheterization, Council on Clinical Cardiology, and the Council on Cardiovascular Radiology and Intervention: endorsed by the American College of Cardiology Foundation, the North American Society for Cardiac Imaging, and the Society for Cardiovascular Magnetic Resonance. *Circulation*. 2007;116:2878–2891.
10. Martin ET, Coman JA, Shellock FG, Pulling CC, Fair R, Jenkins K. Magnetic resonance imaging and cardiac pacemaker safety at 1.5-Tesla. *J Am Coll Cardiol*. 2004;43:1315–1324.
11. Mollerus M, Albin G, Lipinski M, Lucca J. Magnetic resonance imaging of pacemakers and implantable cardioverter-defibrillators without specific absorption rate restrictions. *Europace*. 2010;12:947–951.
12. Baker KB, Tkach JA, Nyenhuis JA, Phillips M, Shellock FG, Gonzalez-Martinez J, Rezai AR. Evaluation of specific absorption rate as a dosimeter of MRI-related implant heating. *J Magn Reson Imaging*. 2004; 20:315–320.
13. Karamitsos TD, Francis JM, Myerson S, Selvanayagam JB, Neubauer S. The role of cardiovascular magnetic resonance imaging in heart failure. *J Am Coll Cardiol*. 2009;54:1407–1424.
14. McCrohon JA, Prasad SK, McKenna WJ, Lorenz CH, Coats AJS, Pennell DJ. Differentiation of heart failure related to dilated cardiomyopathy and coronary artery disease using galinium-enhanced cardiovascular magnetic resonance. *Circulation*. 2003;108:54–59.
15. Kim RJ, Fieno DS, Parrish TB, Harris K, Chen EL, Simonetti O, Bundy J, Finn JP, Klocke FJ, Judd RM. Relationship of MRI delayed contrast enhancement to irreversible injury, infarct age, and contractile function. *Circulation*. 1999;100:1992–2002.
16. Nazarian S, Bluemke DA, Lardo AC, Zviman MM, Watkins SP, Dickfeld TL, Meininger GR, Roguin A, Calkins H, Tomaselli GF, Weiss RG, Berger RD, Lima JAC, Halperin HR. Magnetic resonance assessment of the substrate for inducible ventricular tachycardia in nonischemic cardiomyopathy. *Circulation*. 2005;112:2821–2825.
17. Wu KC, Weiss RG, Thiemann DR, Kitagawa K, Schmidt A, Dalal D, Lai S, Bluemke DA, Gerstenblith G, Marbán E, Tomaselli GF, Lima JA. Late gadolinium enhancement by cardiovascular magnetic resonance heralds an adverse prognosis in nonischemic cardiomyopathy. *J Am Coll Cardiol*. 2008;51:2414–2421.
18. Tandri H, Castillo E, Ferrari VA, Nasir K, Dalal D, Bomma C, Calkins H, Bluemke DA. Magnetic resonance imaging of arrhythmogenic right ventricular dysplasia: sensitivity, specificity, and observer variability of fat detection versus functional analysis of the right ventricle. *J Am Coll Cardiol*. 2006;48:2277–2284.
19. Roes SD, Borleffs CJ, van der Geest RJ, Westenberg JJ, Marsan NA, Kaandorp TA, Reiber JH, Zeppenfeld K, Lamb HJ, de Roos A, Schalij MJ, Bax JJ. Infarct tissue heterogeneity assessed with contrast-enhanced MRI predicts spontaneous ventricular arrhythmia in patients with ischemic cardiomyopathy and ICD. *Circ Cardiovasc Imaging*. 2009;2:183–190.
20. Cobelli FD, Pieroni M, Esposito A, Chimenti C, Belloni E, Mellone R, Canu T, Perseghin G, Gaudio C, Maseri A, Frustaci A, Maschio AD. Delayed gadolinium-enhanced cardiac magnetic resonance in patients with chronic myocarditis presenting with heart failure or recurrent arrhythmias. *J Am Coll Cardiol*. 2006;47:1649–1654.
21. Cheong BYC, Muthupillai R, Wilson JM, Sung A, Huber S, Amin S, Elayda MA, Lee VV, Flamm SD. Prognostic significance of delayed-enhancement magnetic resonance imaging: survival of 857 patients with and without left ventricular dysfunction. *Circulation*. 2009;120:2069–2076.
22. Bogun FM, Desjardins B, Good E, Gupta S, Crawford T, Oral H, Ebinger M, Pelosi F, Chugh A, Jongnarangsin K, Morady F. Delayed-enhanced magnetic resonance imaging in nonischemic cardiomyopathy: utility for identifying the ventricular arrhythmia substrate. *J Am Coll Cardiol*. 2009;53:1138–1145.
23. Desjardins B, Crawford T, Good E, Oral H, Chugh A, Pelosi F, Morady F, Bogun F. Infarct architecture and characteristics on delayed enhanced magnetic resonance imaging and electroanatomic mapping in patients with postinfarction ventricular arrhythmia. *Heart Rhythm*. 2009;6:644–651.
24. Schueler BA, Parrish TB, Lin JC, Hammer BE, Pangrle BJ, Ritenour ER, Kucharczyk J, Truwit CL. MRI compatibility and visibility assessment of implantable medical devices. *J Magn Reson Imaging*. 1999;9:596–603.
25. Suh JS, Jeong EK, Shin KH, Cho JH, Na JB, Kim DH, Han CD. Minimizing artifacts caused by metallic implants at MR imaging: experimental and clinical studies. *AJR Am J Roentgenol*. 1998;171:1207–1213.
26. Stradiotti P, Curti A, Castellazzi G, Zerbi A. Metal-related artifacts in instrumented spine: techniques for reducing artifacts in CT and MRI: state of the art. *Eur Spine J*. 2009;18:102–108.
27. DiFilippo FP, Brunken RC. Do implanted PM leads and ICD leads metal-related artifact in cardiac PET/CT? *J Nucl Med*. 2005;46:436–443.
28. Eggers G, Rieker M, Kress B, Fiebach J, Dickhaus H, Hassfeld S. Artifacts in magnetic resonance imaging caused by dental material. *MAGMA*. 2005;18:103–111.

CLINICAL PERSPECTIVE

The decision to perform cardiac magnetic resonance (CMR) imaging in patients with cardiac pacemakers (PMs) and implantable cardioverter-defibrillator (ICDs) depends on the balance of risks versus benefits of imaging in each individual. Although considerable work has focused on safety considerations, this work evaluated the potential limitations imposed on CMR by susceptibility artifacts in patients with PM/ICDs. In patients with left-sided PM and right-sided PM/ICD systems, CMR images had minimal artifacts regardless of the image sequence and were completely interpretable. In contrast, in patients with left-sided ICD/biventricular (BiV)-ICD systems, artifact effects on late gadolinium-enhanced (LGE)-CMR were greater than those on MR angiography, cine, T2-weighted, and perfusion CMR. We found it particularly difficult to evaluate the anterior and apical regions on LGE-CMR of patients with left-sided ICD/BiV-ICD systems. Lower body mass index, larger generator size, larger left ventricular end-diastolic diameter, and shorter distance between the PM/ICD generator and the cardiac silhouette on chest radiography are associated with greater artifact size on CMR. The results of this study may improve patient selection for CMR in the setting of PM/ICD systems.

Circulation
Cardiovascular Imaging

Quantitative Assessment of Artifacts on Cardiac Magnetic Resonance Imaging of Patients With Pacemakers and Implantable Cardioverter-Defibrillators

Takeshi Sasaki, Rozann Hansford, Menekhem M. Zviman, Aravindan Kolandaivelu, David A. Bluemke, Ronald D. Berger, Hugh Calkins, Henry R. Halperin and Saman Nazarian

Circ Cardiovasc Imaging. 2011;4:662-670; originally published online September 23, 2011;
doi: 10.1161/CIRCIMAGING.111.965764
Circulation: Cardiovascular Imaging is published by the American Heart Association, 7272 Greenville Avenue, Dallas, TX 75231

Print ISSN: 1941-9651. Online ISSN: 1942-0080

Supplemental Table. Artifacts on Cine CMR

	ICD / BiV-ICD N=56 Scans	PM N=15 Scans	P-Value
% of Scans with Any Artifact on Cine CMR			
Short Axis	100% (56 / 56)	93.3% (14 / 15)	0.211
Horizontal Long Axis	26.9% (14 / 52)	23.1% (3 / 13)	1.0
Vertical Long Axis	76.1% (35 / 46)	33.3% (4 / 12)	0.012
Artifacts Size on Cine CMR [cm^2]			
Short Axis	197.2±31.2	89.0±25.0	<0.0001
Horizontal Long Axis	105.3±61.2	35.6±9.1	0.001
Vertical Long Axis	189.2±57.0	66.1±30.3	0.0002

Values are shown as percentage (N) and mean ± SD.

CMR=cardiac magnetic resonance; ICD=implantable cardioverter defibrillator; BiV-ICD=biventricular ICD; PM=pacemaker.

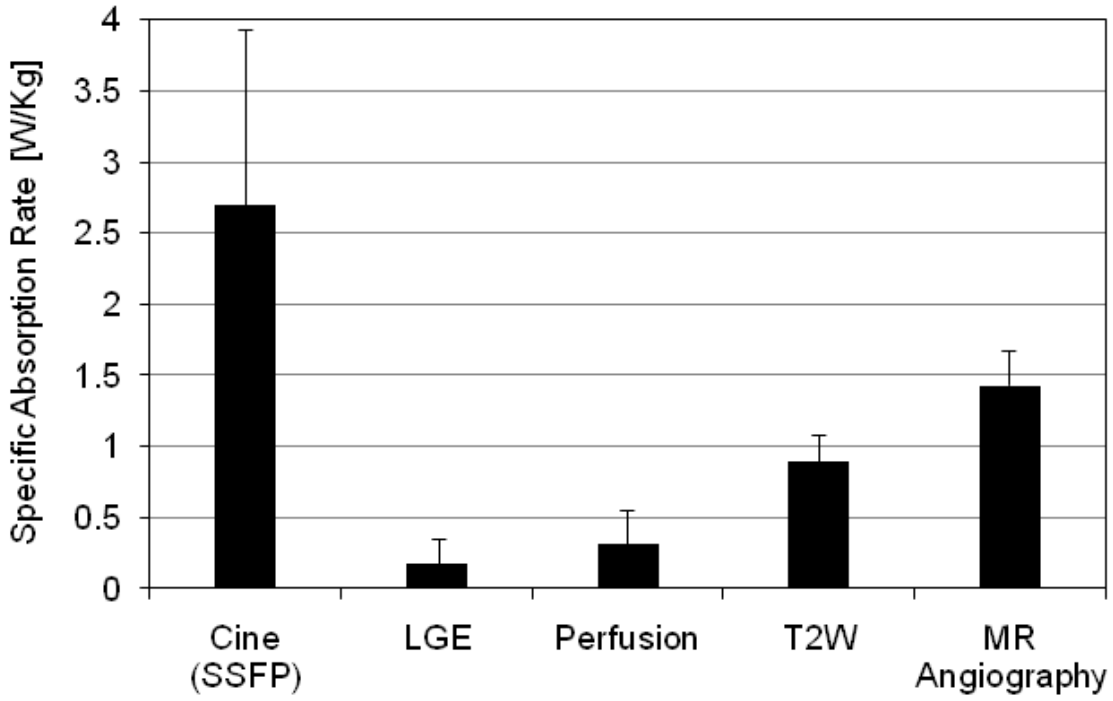

Supplemental Figure 1. Estimated Whole-Body Averaged Specific Absorption Rate (SAR) for Each Image Sequence

The estimated whole-body averaged SAR was less than 2.0 W/Kg in most image acquisition sequences except SSFP cine cardiac magnetic resonance.

SSFP=steady state free precession; LGE=late gadolinium enhanced; T2W=T2-weighted; MR=magnetic resonance.

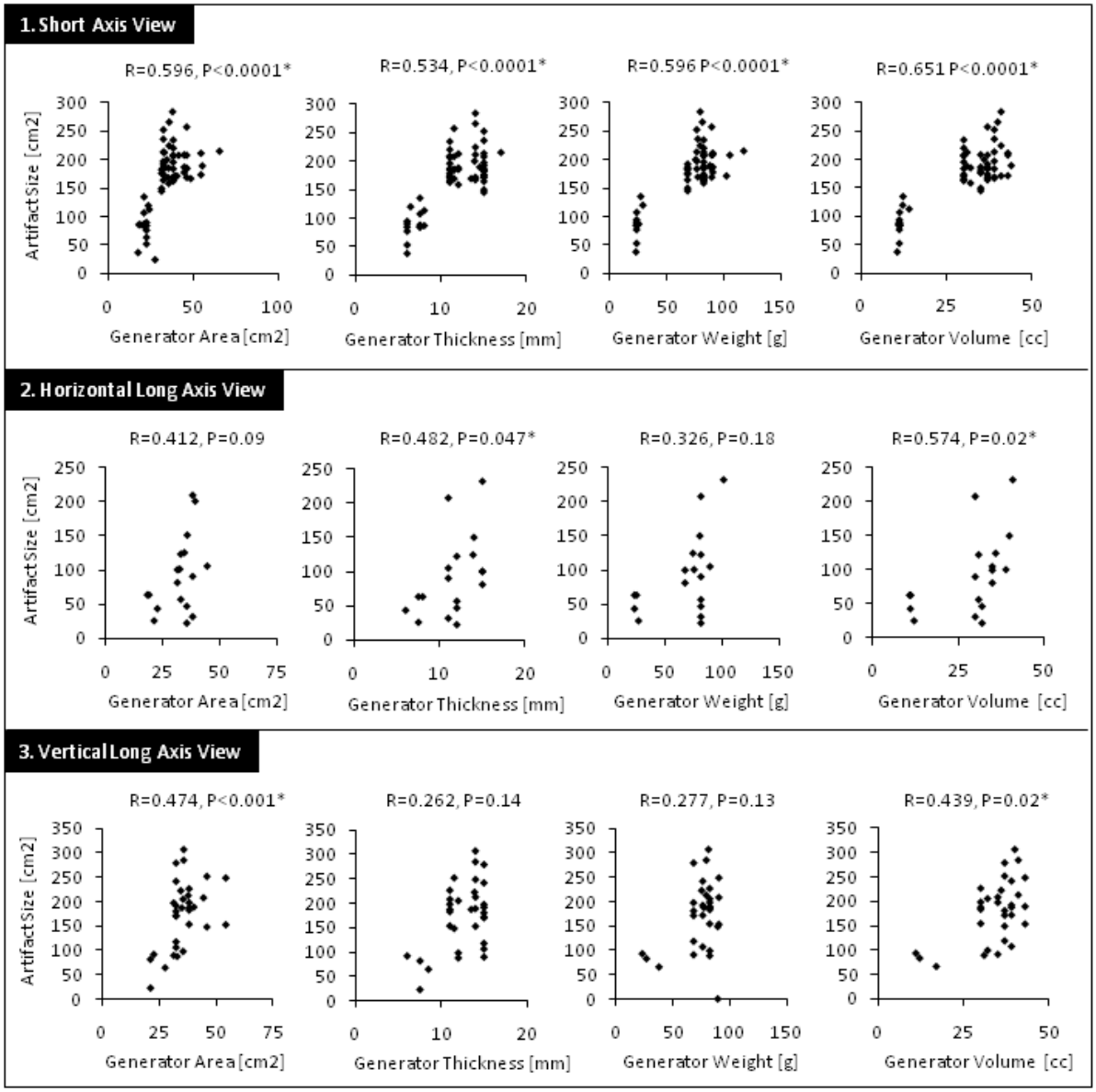

Supplemental Figure 2. Correlation of Artifact Size on Cine CMR and Generator Dimension.

The association of artifact size on cine CMR and generator dimensions including area [cm2], thickness [mm], weight [g] and volume [ml] were demonstrated with Spearman correlation analysis in SA, HLA and VLA planes, respectively. The strongest correlation was observed in SA planes.

Significant P-value defined as P<0.05 are shown by the asterisk (*).

SA = short axis; HLA = horizontal long axis; VLA = vertical long axis.

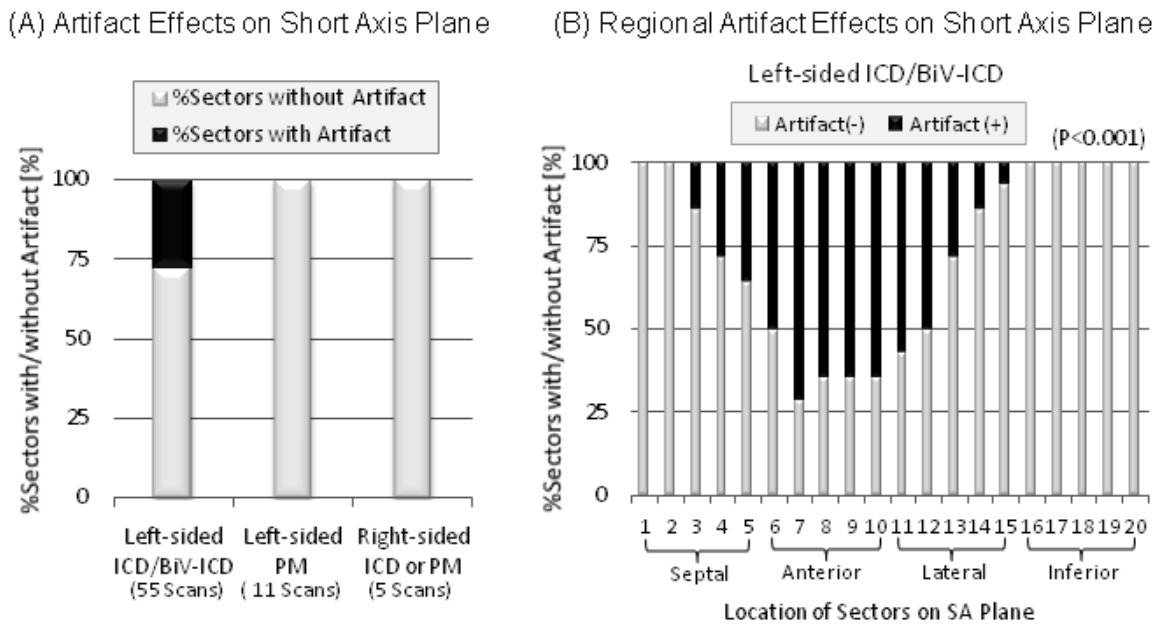

Supplemental Figure 3. (A) Artifact effects in short axis plane of cine CMR due to the generator were quantitatively assessed in patients with left and right-sided ICD/BiV-ICD or PM systems. Artifacts on cine CMR were only observed in patients with left-sided ICD/BiV. (B) Details about the regional artifact effects on short axis plane were demonstrated in patients with left-sided ICD/BiV-ICD.A majority of the artifacts on cine CMR were observed in the anterior regions.